Dhaka Univ. J. Sci. 58(2): 297-300, 2010 (July)

Scaling Rules to Understand Current Limiting Mechanisms in High Temperature Superconductors

Mitul Anwar Chowdhury

IER, Dhaka University, Dhaka-1000, Bangladesh

Received on 20.12.2009. Accepted for Publication on 31.05.2010.

Abstract

An important property of high temperature superconducting conductors is their critical current density $J_c(H)$. We seek regularities in the $I_c(H)$ curves of Ag/(Bi, Pb)$_2$Sr$_2$Ca$_2$Cu$_3$Ox conductors to better understand their current limiting mechanisms (CLM's). Metallurgical variations in Ag/Bi2223 conductors cause changes in $J_c(H)$. One way we can try to understand these changes is by looking for scaling laws for $J_c(H)$. The Kramer model postulates scaling laws and explains reasonably well the relation of $J_c(H)$ at high field in low temperature superconductors. We use the Kramer model and scaling of volume pinning force density for different tapes of high temperature superconductors to arrive at conclusions about the CLM'S in these conductors at high fields.

I. Introduction

In this study the scaling rule of Kramer model is extended for high fields and high temperature superconductor tapes. When the tapes are properly normalized it leads to a uniformity in the curves and suggests important results for current limiting mechanisms.

If a type II superconductor is in an applied transverse magnetic field greater than H_{c1} and if a current is passed through the specimen, there will be a certain transport current density at every point. As the superconductor is in the mixed state, it is threaded by magnetic flux line cores. There will be a Lorentz force (defined as $F_L = I \times B = J \times \Phi_0$) between this flux line and the current. In this case the force acts between the electrons which carrying transport current and the vortices generating magnetic flux. When the vortices or the flux lines form a lattice, they interact with one another and can travel together. If the flux lines move, energy is dissipated and resistance develops.[1,2]

The Lorentz force F_L acts at right angles both to the direction of the transport current and to the magnetic field in each vortex. In most applications the vortices are pinned (that is held in place or kept from moving) on imperfections and interfaces with non-superconducting materials and the resistance will remain zero until the critical current density J_c is exceeded. When the current density is higher than J_c the pinning force is no longer strong enough and vortices start moving. This movement causes a resistance. Flux lines can be kept from moving by forces between defects in the crystal lattice or metallurgical defects in the superconducting material.[12] If a few lines are pinned it is sufficient to prevent all the flux lines from moving. Volume pinning force is the average pinning force per unit length of core. It is known that if the transport current density produces a Lorentz force per unit length of core which is less than F_v , the core lattice will not move but if the transport current is increased, so that the Lorentz force exceeds the volume pinning force F_v, the vortices are no longer pinned which causes flux lines to move and when the vortices move under the influence of such current, the superconductor gets resistance.[10,11] We can get the value of critical current density J_c from the volume pinning force F_v from the important relation $F_v = J_c(H) \times H$. A $J_c(H)$ plot corresponds to the current density as a function of field above which resistance free currents are no longer possible.

$(Bi,Pb)_2Sr_2Ca_2Cu_3O_x$ (Bi-2223) is a high temperature superconductor with T_c of 110K.[8] It is a ceramic type II superconductor. This compound contains the elements bismuth, strontium, calcium, copper and oxygen. Typically, a small amount of lead is also included in this compound to make it more stable. This kind of material is used in superconducting applications to electric power transmission lines, transformers, electromagnets, and motors. The powder-in-tube technique is used to produce Bi-2223 wires and tapes. This process normally consists of two heat treatment steps separated by an intermediate rolling step. Industries are producing kilometer long Bi-2223 wires. Bi-2223 conductors with properties that are essentially constant at length scales to beyond 200 m have been studied.[6] This constancy shows that the leading industries are able to make uniform conductors and have effectively eliminated large-scale manufacturing-induced current-limiting mechanisms. In order to increase J_c it is necessary to minimize the effects of multiple current limiting mechanisms in different field ranges.[9]

II. Scaling

An important property of high temperature superconductors is their critical current $I_c(H)$. We seek regularities in the $I_c(H)$ curves of Ag /(Bi, Pb)$_2$Sr$_2$Ca$_2$Cu$_3$Ox to better understand their current limiting mechanisms. One way we can try to understand these changes of $I_c(H)$ curves is by looking for scaling laws for $J_c(H)$. The Kramer model postulates scaling laws and explains reasonably well the behavior of $J_c(H)$ at high fields in low temperature superconductors. [3,5]

According to Kramer's model the volume pinning force F_v can be discussed in high and low field regions and it is given by Kramer as

$$F_s = \left| \mathbf{J}_c(H) \times \mathbf{H} \right| = K_S h^{1/2}(1-h)^2 \quad \text{in the high field region and ----} \quad (1)$$

$$F_p = \left| \mathbf{J}_c(H) \times \mathbf{H} \right| = K_p h^{1/2}/(1-h)^2 \quad \text{in the low field region ---------} \quad (2)$$

Where $h = H/H_{c2}$,

K_p and K_s are parameters which depend on the details of the pinning interactions in the conductors. K_p is given by $K_p = 5\times10^6 \rho P \omega^4 \beta^4 H_{c2}^{5/2} (\varphi_0^{1/2} K_1^2)^{-1}$ dyn/cm^3 and $K_1$is the Ginsburg-Landau constant ($K_1 = H_{c2}/\sqrt{2}H_c$). The other parameter K_s is related to flux lattice spacing a_0. $K_s = 0.56 H_{c2}^{5/2} K_1^{-2}(1- a_0\sqrt{\rho})^{-2}$.[5] In K_p and K_s, ρ is the density of flux

pinning sites, β and P are constants, and ω is net number of pinning sites per unit length of flux line.

The above equation (1) was derived assuming at high fields flux motion occurs by shear of the flux line lattice around pins too strong to be broken.

For high field behavior of J_c another form of equation (2) is more convenient, which is

$J_c^{1/2}H^{1/4}$ = constant $(H_{c2}- H)$ $[F_v = J_c \times B = J_c \times \mu_o H]$

we derive the equation in the form of

$$F_v \sim h^{1/2}(1-h)^2 \quad \text{at high fields}$$

$$\text{Where, } h=H/H_k \quad \text{but } F_v \sim I_c h$$

Here H_k is defined as a new quantity called the Kramer field for high temperature superconductors and it is different from H_{c2}. The value of H_k is different for each superconducting metal and it depends on temperature and microstructure.

So, $I_c h \sim h^{1/2}(1-h)^2$

$I_c^{1/2} h^{1/4} \sim 1-h$

Since $I_c^{1/2} h^{1/4}$ is a linear function of 1-h this equation can be used to determine H_k by plotting $I_c^{1/2} H^{1/4}$ against H and extrapolating to the horizontal axis.

This extrapolation has been used to find H_{c2} of low temperature superconductors. Here we apply it to high temperature superconductors and we will show that the Kramer model explains reasonably well the behavior of $I_c^{1/2} H^{1/4}$ at high fields as this function is a straight line through most of the field region. The Kramer model indicates that at high fields $J_c(H)$ is due to the shear of the flux line lattice around strong pins.[3] So, it means if the pin are sufficiently strong $J_c(H)$ depends more on properties of the flux line lattice at high fields.

Another important study is to see the nature of pinning force density as a function of magnetic field. So, the field dependence of the volume pinning force F_v is an important measurement of flux pinning in a high field superconductor.

The shape of the $F_v(H)$ curve is important because it can indicate what the elementary flux pinning mechanism is and what the defects in the microstructure are that cause the pinning. For better understanding of these mechanisms we used scaling rules. Our interest in this discussion is to see if there is a uniform pattern for both the Kramer function F_k $(=I_c^{1/2}(\mu_0 H)^{1/}4)$ and the volume pinning force F_v. If the $F_k(H)$ and $F_v(H)$ curves do scale this scaling suggests there is a single mechanism determining J_c in all the samples.

III. Experimental Procedure

Tapes are produced by means of a thermo mechanical process in which the tape is heated to various temperatures for various times and undergoes various mechanical processes. Some of the tapes that are used for data analysis were collected from the University of Wisconsin-Madison and some were provided by another manufacturer. Bi2223 tapes were made using the powder in tube process.[4,6] Precursor powders of Bi2223 were packed into Ag tube and annealed in N_2 for 2 to 12 hours. The tubes were reduced to 2.0 mm in diameter, which were then rolled to 150μm thick tapes. The first heat treatments were done at 825^0C in a flowing 7.5% O_2/balance N_2 atmosphere. Tape thickness was then reduced by rolling between two rollers of the diameter 152 mm after the first heat treatment. Tapes were heat treated for an additional 24 hours at 827^0C, 48 hours at 822^0C and 24 hours at 805^0C. The specimens were designated as UWB 130. There were six heat treatments at different dwell temperature from 750^0C to 800^0C in steps of 10^0C. Each heating ramp included a heating rate of 5^0C/min from 50^0C to dwell temperature. After that each sample was cooled at a rate of 2^0C/min back down to 50^0C. V-I characteristics were obtained using a standard four probe technique at different magnetic fields generally from 0 to 600 mT. at 77K with applied magnetic field perpendicular to the tape surface then $I_c(H)$ was extracted using the criterion of 1μV/cm. These data were changed to critical current density, J_c by dividing the critical current by the cross sectional area of the wires which was measured previously.

IV. Computational Methods

V-I Characteristics of 12 optimized (Bi,Pb)SrCaCuO/Ag multifilamentary tapes from different manufacturers were studied and $J_c(H)$ was obtained. All data was provided by Dr Louis Schwartzkopf and was taken at the Applied Superconductivity Center University of Wisconsin Madison.[7]

The data that are analyzed consisted of current-voltage curves in applied magnetic field generally from 0 to 600 mT. For each curve the offset voltage (the voltage when I=0) was determined and subtracted off using a transformation in Sigma Plot. Then $I_c(H)$ was determined using the criterion for I_c of 1 μV/cm. So if the voltage tapes are 1cm apart then the criterion is 1μV. For our BSCCO conductors, the tapes were 0.6 cm apart so the criterion is 0.6 μV. So I_c was taken to be the current at which the voltage first reached 0.6 μV and was found by using the interpolation function in Sigma Plot.

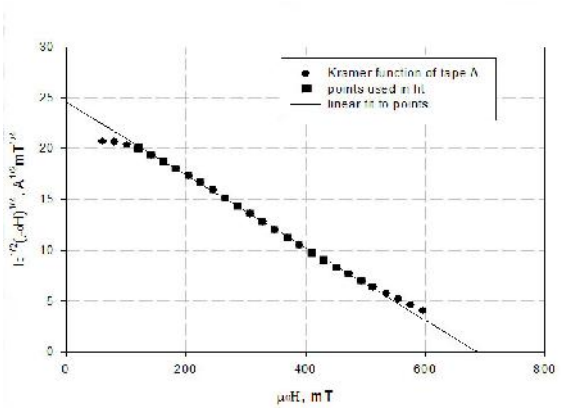

Fig.1. Kramer plot of tape A

V. Results

The Kramer function $F_k(=I_c^{1/2}(\mu_0 H)^{1/4})$ was plotted vs H for all 14 samples. On the vertical axis we plot $I_c^{1/2}(\mu_0 H)^{1/4}$ with units of $(A)^{1/2}(mT)^{1/4}$ and on the horizontal axis it is $\mu_0 H$ in tesla for each sample. $I_c^{1/2}(\mu_0 H)^{1/4}$ is defined as $F_k(H)$. This kind of curve is known as a Kramer plot. One typical graph of tape A is shown in fig(1). This graph has three regions. At low fields and high fields it deviates from a straight line

but from around 150mT to 500mT it is fairly close to a straight line. The linear portion of the graph is found by inspection. H_k is found by using the Regression Function in Sigma Plot for the linear portion. The H_k value is determined from the horizontal intercept.

Kramer plots of the six samples from the outside manufacturer were plotted on the same set of axes, Fig(2). This gives a similar pattern of curves but the deviation from sample to sample at 60mT, the lowest field measured is from 20 to 25 $(A)^{1/2}(mT)^{1/4}$ which is about a 20% variation. At the highest field measured 600 mT the variation is from 4 to 7 $(A)^{1/2}(mT)^{1/4}$ which is about 42%. So we see that in unnormalized Kramer plot there is significant variation of $F_k(H)$ from sample to sample.

Next the graphs of $F_k(H)$ are replotted with the axes scaled. The six specimens are normalized on the same set of axes. In order to normalize on the X-axis we plot $h = H/H_k$; that is, we set the scale so that h=1 when H= H_k. Using regression, H_k is calculated from the value of the slope and the y- intercept. After that $I_c^{1/2}(\mu_0 H)^{1/4}$ at ½ H_k is found. For the Y axis we set the scale so that $I_c^{1/2}(\mu_0 H)^{1/4} = ½$, when h= ½. Then F_k normalized vs H normalized is plotted for all samples on the same set of axes. This gives us normalized Kramer plots. Fig(3) shows the normalized Kramer plots. From graph 3 we see that all the curves fall onto a single curve in the normalized plot. This suggests that what determines the critical current density $J_c(H)$ for these tapes is the same. In other words, the current limiting mechanism is the same for all these tapes.

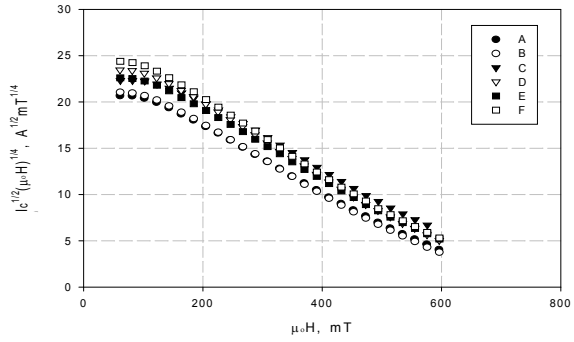

Fig. 2. Unnormalized Kramer plot of the six samples from the outside manufacturer

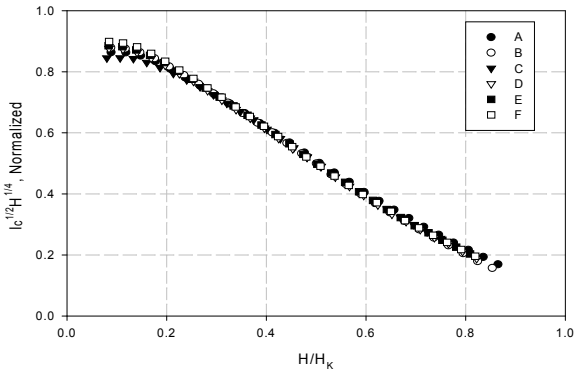

Fig. 3. Normalized Kramer plot of the six samples from the outside manufacturer

Same procedure is used with six other samples which are produced at the University of Wisconsin-Madison and here labeled as G, H, I, J, K, L. For these samples I_c is obtained at fields from 0 to 320 mT so for these samples data is obtained over a smaller range of field than the previous set of samples. When all the six samples are plotted on the same set of axes the Kramer function varies by about 14% at the lowest field measured and about 17% at the highest field. Figure (4) is the unnormalized Kramer plot. After normalization of both axes, same way as it was done for the previous samples it is found that all the curves collapse into one curve except for some deviation at low fields. This collapse signifies the universality of the scaling law. Figure (5) is showing how all the curves collapse into one.

We see that $F_k(H)$is linear in H over a reasonably wide range of H. So our two sample sets

1) showed linear dependence of $I_c^{1/2}H^{1/4}$ on H and
2) allowed us to find H_k from the slope of $I_c^{1/2}(\mu_0 H)^{1/4}$ vs H

As our plots are straight lines with H over a wide range in magnetic field, this implies that the distance between the pinning sites in these wires is considerably larger than the flux lattice spacing a_0. In table (1) data for H_k values of the 12 tapes are listed.

Although the values of H_k obtained by extrapolation differ, after normalization for six samples from the outside manufacturer, we see that different samples fall on a single curve. This implies the validity of scaling law. However from fig(5) we can see

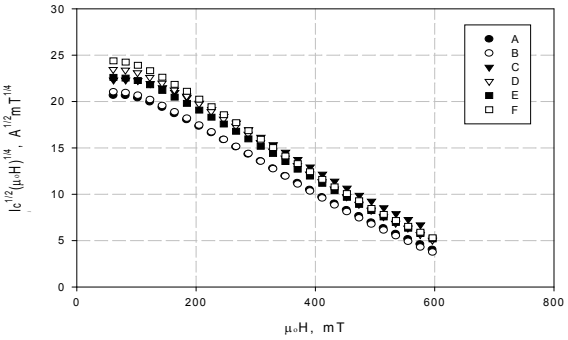

Fig. 4. Unnormalized Kramer plot of the six UWM Samples

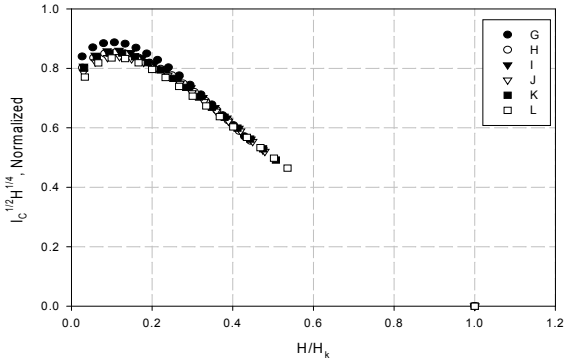

Fig. 5. Normalized Kramer plot of the six UWM samples

that not all portions of the graph are in a straight line. We can divide the graph in three regions. In first region which is at low field F_k falls off rapidly. This may be due to weak link breaking at low fields. In the next region between fields of 180mT to 400mT (which is the largest portion of the graph) F_k falls off linearly. Finally at highest fields F_k falls off rather slower than linearly compared to the intermediate field region. At higher fields, where all weak links are broken and the remaining current carrying cross section is constant $F_k(h)$ is same for all tapes to within a proportionality constant. This illustrates its use in analyzing the magnetic field dependence of the critical current density. I also calculated the volume pinning force F_v (=I_cH) for all the samples. The volume pinning force F_v is actually defined as $F_v = J_cB$. Normalized pinning force was plotted as a function of reduced magnetic field (reduced to H_k) for six UWM samples and six samples from the outside manufacturer. On the vertical axis we have F_p/ F_{pmax}. Here F_{pmax} is the maximum pinning force observed for each sample. In the horizontal axis H/H_k was plotted. The H_k value used here is same that is found from the Kramer plot. The peak in the pinning force as a function of h is a universal feature of pinning in all hard superconductors.[3] Data for different samples fall on a single curve when normalized in this way and if the normalized data can be described by a single curve, then the same mechanism determines F_v for all the samples. In Fig (6) & fig(7) are such pinning curves. We can see that pinning curves of 6 samples from outside manufactures and six UWM samples both fall onto a single curve when normalized.

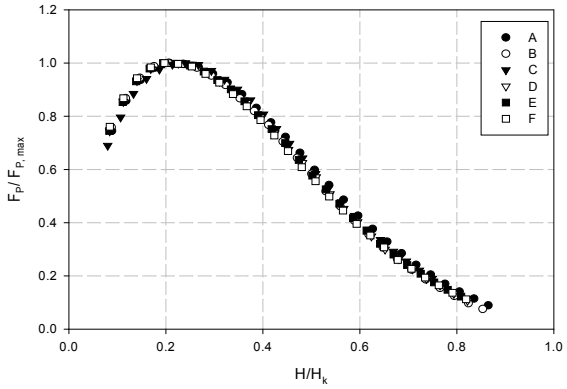

Fig. 6. Pinning plot of the six samples from the outside manufacturer

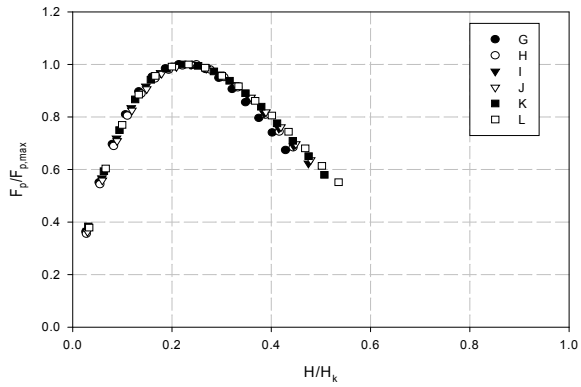

Fig. 7. Pinning plot of the six UWM samples

Table. 1. Value of the Characteristic field H_k for all samples

Tape	Characteristic field H_k(mT)
A	689
B	699
C	769
D	725
E	737
F	728
G	767
H	740
I	692
J	686
K	649
L	614

VI. Conclusion

This study is based on a scaling rule proposed by Kramer. Our finding is to see how this scaling rule works at high fields for high temperature superconductors and what happens if all the samples are properly normalized. Graphs of $I_c^{1/2}(\mu_0 H)^{1/4}$ versus H are approximately linear in most of the field region and Kramer's model applies reasonably well for these B2223 tapes. After proper normalization of each set samples on the same set of axes, all samples collapse onto a single curve. This result is important because it suggests that what determines $J_c(H)$ for these tapes is the same. So the current limiting mechanism is the same for all these tapes.

Volume pinning force F_v (=I_cH) for all the samples were calculated. Data for different samples in each sample set fell onto a single curve when normalized. This suggests that the mechanism that determines the volume pinning force is the same for all the specimens studied.

---

1. Vladimir Z. Kresin and Stwart A. Wolf, Fundamentals of Superconductivity, Kluwer Academic / Plenum Publishers, 1990, 4
2. Rose-Innes A. C, and E.H Rhoderick, Introduction to Superconductivity, second edition, Pergamon Press, 1978, 19
3. Edward J. Kramer, J.Appl.Phys. **44**, March, (1973),1360-1369.
4. Lance David Cooley, PhD Thesis, University of Wisconsin-Madison, (1993)
5. Suenaga M., Superconductor Materials Science, Edited by Simon Forner and Brian B. Schwartz, Plenum press, 145-251
6. Jermal G. Chandler, M.S Thesis, University of Wisconsin-Madison, (2002)
7. Applied Superconductivity Center, April 12 2004, http://www.asc.wisc.edu/bscco/bscco.htm
8. Lotte Gottschalck Andersen, Structural Properties of Superconducting Bi-2223/Ag Tapes, April 17 2004, http://www.risoe.dk/rispubl/AFM/afmpdf/ris-r-1271.pdf
9. L.A. Schwartzkopf, J.Jiang, X.Y. Cai, D. Apodaca, and D.C. Larbalestier, Applied Physics Letters, **75**, (1999), 3168-3170
10. Y. Mawatari, H. Yamasaki, S. Kosaka and M. Umeda, Cryogenics **35**, (1995), 161-167
11. Thomas P. Sheahen, Introduction to High-Temperature Superconductivity, Plenum press, New York, NY, 1994
12. Charles Kittel, Introduction to Solid State Physics, 6th edition, John Wiley & Sons Inc., New York, Ny, 1986